to a separate drop of PBS to prevent cross-contamination of sperm from different organs. The sperm from each organ were then removed with insect pins and minimal manipulation. Slides to be scored for GFP vs non-GFP sperm were dissected in 0.5 $\mu g\,ml^{-1}$ DAPI (4,6-diamidino-2-phenylindole) in PBS, covered immediately with a coverslip and scored with an epifluorescent microscope within 2 h of dissection. Slides that required only simple sperm counts were dried after dissection at 60 °C for 5–10 min, fixed in 3:1 methanol and glacial acetic acid for 5 min, rinsed three times in PBS and labelled with DAPI in glycerol (0.5 $\mu g\,ml^{-1}$). All sperm in each of the three storage organs of every female were counted. To ensure precision, 10% of the slides were counted at least twice by different people.

Egg hatchability. Females were allowed to lay eggs on small plastic spoons filled with grape-juice-tinted medium for 24 h, and then either transferred to a fresh spoon or discarded. Spoons were stored at 24 °C for 28 h before hatched and unhatched eggs were counted. Brown eggs, which may indicate zygotes that died early in development, were observed only rarely.

Received 3 March; accepted 28 May 1999.

1. Smith, R. L. (ed.) *Sperm Competition and the Evolution of Animal Mating Systems* (Academic, London, 1984).
2. Birkhead, T. R. & Møller, A. P. (eds.) *Sperm Competition and Sexual Selection* (Academic, London, 1998).
3. Parker, G. A. Sperm competition and its evolutionary consequences in the insects. *Biol. Rev.* **45,** 525–567 (1970).
4. Eberhard, W. G. *Female Control: Sexual Selection by Cryptic Female Choice* (Princeton Univ. Press, Princeton, 1996).
5. Birkhead, T. R. & Møller, A. P. *Sperm Competition in Birds: Evolutionary Causes and Consequences* (Academic, London, 1992).
6. Simmons, L. W. & Siva-Jothy, M. T. in *Sperm Competition and Sexual Selection* (eds Birkhead, T. R. & Møller, A. P.) 341–434 (Academic, London, 1998).
7. Nonidez, J. F. The internal phenomena of reproduction in Drosophila. *Biol. Bull.* **39,** 207–230 (1920).
8. Lobashov, M. E. Mixture of sperm in case of polyandry in *Drosophila melanogaster. C. R. (Doklady) Acad. Sci. de l'URSS* **23,** 827–830 (1939).
9. Kaufmann, B. P. & Demerec, M. Utilization of sperm by the female *Drosophila melanogaster. Am. Nat.* **76,** 445–469 (1942).
10. Lefevre, G. & Jonsson, U. B. Sperm transfer, storage, displacement, and utilization in *Drosophila melanogaster. Genetics* **47,** 1719–1736 (1962).
11. Newport, M. E. A. & Gromko, M. H. The effect of experimental design on female receptivity to remating and its impact on reproductive success in *Drosophila melanogaster. Evolution* **38,** 1261–1272 (1984).
12. Scott, D. & Richmond, R. C. Sperm loss by remating *Drosophila melanogaster* females. *J. Insect Physiol.* **36,** 451–456 (1990).
13. Scott, D. & Williams, E. Sperm displacement after remating in *Drosophila melanogaster. J. Insect Physiol.* **39,** 201–206 (1993).
14. Harshman, L. G. & Prout, T. Sperm displacement without sperm transfer in *Drosophila melanogaster. Evolution* **48,** 758–766 (1994).
15. Gilchrist, A. S. & Partridge, L. Male identity and sperm displacement in *Drosophila melanogaster. J. Insect Physiol.* **41,** 1087–1092 (1995).
16. Gromko, M. H., Gilbert, D. G. & Richmond, R. C. in *Sperm Competition and the Evolution of Animal Mating Systems* (ed. Smith, R. L.) 371–426 (Academic, London, 1984).
17. Imhof, M., Harr, B., Brem, G. & Schlötterer, C. Multiple mating in wild *Drosophila melanogaster* revisited by microsatellite analysis. *Mol. Ecol.* **7,** 915–917 (1998).
18. Gromko, M. H. & Markow, T. A. Courtship and remating in field populations of *Drosophila*. *Anim. Behav.* **45,** 253–262 (1993).
19. Gromko, M. H., Newport, M. E. A. & Kortier, M. G. Sperm dependence of female receptivity to remating in *Drosophila melanogaster. Evolution* **38,** 1273–1282 (1984).
20. Santel, A., Winhauer, T., Blümer, N. & Renkawitz-Pohl, R. The *Drosophila don juan* (*dj*) gene encodes a novel sperm specific protein component characterized by an unusual domain of a repetitive amino acid motif. *Mech. Dev.* **64,** 19–30 (1997).
21. Snedecor, G. W. & Cochran, W. G. *Statistical Methods* (Iowa State Univ. Press, Ames, 1967).
22. Sokal, R. R. & Rohlf, F. J. *Biometry* (Freeman, New York, 1995).
23. Nachtsheim, H. Eine Method zur Prüfung der Lebendauer genotypisch verschiedener Spermien bei Drosophila. Verhandl. V. Intern. Kongr. Verebungsw., 1143–1147. *Z. Ind. Abst. Vereb* (Suppl. II) (1927).
24. Rice, W. R. Sexually antagonistic male adaptation triggered by experimental arrest of female evolution. *Nature* **381,** 232–234 (1996).
25. Clark, A. G. & Begun, D. J. Female genotypes affect sperm displacement in Drosophila. *Genetics* **149,** 1487–1493 (1998).
26. Clark, A. G., Begun, D. J. & Prout, T. Female × male interactions in *Drosophila* sperm competition. *Science* **283,** 217–220 (1999).
27. Price, C. S. C. Conspecific sperm precedence in Drosophila. *Nature* **388,** 663–666 (1997).
28. Coyne, J. A., Aulard, S. & Berry, A. Lack of underdominance in a naturally occurring pericentric inversion in *Drosophila melanogaster* and its implications for chromosome evolution. *Genetics* **129,** 791–802 (1991).
29. Ingman-Baker, J. & Candido, E. P. Proteins of the *Drosophila melanogaster* male reproductive system: two-dimensional gel patterns of proteins synthesized in the XO, XY, and XYY testis and paragonial gland and evidence that the Y chromosome does not code for structural sperm proteins. *Biochem. Genet.* **18,** 809–828 (1980).
30. Kiefer, B. I. Ultrastructural abnormalities in developing sperm of X/O *Drosophila melanogaster. Genetics* **54,** 14441–1452 (1966).

Acknowledgements. We thank M. DeAngelis, C. Gronlund, C. Kim, C. Mercader, J. Posluszny and A. Travelli for technical assistance; A. Santel for the *dj*GFP II/Cyo flies; A. James and R. Snook for miscellaneous help; B. Robbins for supplies; and A. Civetta, T. Prout and C.-I. Wu for comments. This work was supported by an NSF predoctoral fellowship, NIH genetics training grant and NSF doctoral dissertation improvement grant to C.S.C.P. and by an NIH grant to J.A.C.

Correspondence and requests for materials should be addressed to J.A.C. (e-mail: j-coyne@uchicago.edu).

Vanilloid receptors on sensory nerves mediate the vasodilator action of anandamide

Peter M. Zygmunt*†, Jesper Petersson†, David A. Andersson†, Huai-hu Chuang‡, Morten Sørgård†, Vincenzo Di Marzo§, David Julius‡ & Edward D. Högestätt*†

† *Department of Clinical Pharmacology, Institute of Laboratory Medicine, University of Lund, S-221 85 Lund, Sweden*

‡ *Department of Cellular and Molecular Pharmacology, University of California, San Francisco, California 94143-0450, USA*

§ *C.N.R. Instituto per la Chimica di Molecole di Interesse Biologico, Via Toiano 6, Arco Felice, Napoli 80072, Italy*

* *These authors contributed equally to this work*

The endogenous cannabinoid receptor agonist anandamide[1] is a powerful vasodilator of isolated vascular preparations[2–4], but its mechanism of action is unclear. Here we show that the vasodilator response to anandamide in isolated arteries is capsaicin-sensitive and accompanied by release of calcitonin-gene-related peptide (CGRP). The selective CGRP-receptor antagonist 8-37 CGRP (ref. 5), but not the cannabinoid CB1 receptor blocker SR141716A (ref. 7), inhibited the vasodilator effect of anandamide. Other endogenous (2-arachidonylglycerol, palmitylethanolamide) and synthetic (HU 210, WIN 55,212-2, CP 55,940) CB1 and CB2 receptor agonists[1] could not mimic the action of anandamide. The selective 'vanilloid receptor' antagonist capsazepine[6,7] inhibited anandamide-induced vasodilation and release of CGRP. In patch-clamp experiments on cells expressing the cloned vanilloid receptor (VR1)[8], anandamide induced a capsazepine-sensitive current in whole cells and isolated membrane patches. Our results indicate that anandamide induces vasodilation by activating vanilloid receptors on perivascular sensory nerves and causing release of CGRP. The vanilloid receptor may thus be another molecular target for endogenous anandamide, besides cannabinoid receptors, in the nervous and cardiovascular systems.

Anandamide (arachidonylethanolamide) was originally isolated from brain as an endogenous cannabinoid receptor ligand[9]. Biosynthetic pathways for anandamide are also present outside the central nervous system, for example, in vascular endothelium and macrophages[10,11]. It has been suggested that anandamide induces hypotension in anaesthetized rats by inhibiting peripheral sympathetic neurotransmission[12]. Macrophage-derived anandamide is implicated in haemorrhagic shock[13] and endotoxin-induced hypotension[14]. Although CB1 receptor messenger RNA has been detected in sympathetic nerves, vascular endothelium and smooth muscle[10,15,16], the involvement of cannabinoid receptors in the vasodilator effects of anandamide in isolated vascular preparations has been questioned[2,4,17]. Anandamide is structurally related to capsaicin and olvanil (*N*-vanillyloleamide), compounds that all have an amide bond and an aliphatic side chain. Capsaicin and olvanil activate a subpopulation of primary sensory neurons, which can then become refractory to subsequent stimuli (desensitization)[7]. As such nerves mediate vasodilation[18], we hypothesized that the vascular effects of anandamide and capsaicin have a common mechanism, involving excitation of primary sensory nerves in the vessel wall and consequent release of vasodilator neuropeptides such as CGRP.

To test this proposal, we examined the effects of capsaicin and the selective CGRP-receptor antagonist 8-37 CGRP (ref. 5) on anandamide-induced relaxation in rat hepatic and small mesenteric arteries and guinea-pig basilar artery. Pretreatment with capsaicin to cause desensitization and/or neurotransmitter depletion in perivascular sensory nerves abolished anandamide-induced relaxation in all

three arteries (Fig. 1a, b). 8-37 CGRP also inhibited the response to anandamide (Fig. 1c). As shown in the rat hepatic artery, the relaxation induced by exogenous CGRP was unaffected by pretreatment with capsaicin (10 μM), whereas 8-37 CGRP (2 μM) caused a significant rightward parallel shift of the concentration–relaxation curve for CGRP (control: $pEC_{50} = 9.56 \pm 0.04$, $E_{max} = 100 \pm 1\%$; capsaicin: $pEC_{50} = 9.51 \pm 0.02$, $E_{max} = 100 \pm 1\%$; 8-37 CGRP: $pEC_{50} = 8.54 \pm 0.13$, $E_{max} = 100 \pm 1\%$; $n = 6$).

At a concentration that induced vasodilation, anandamide elicited significant release of CGRP and an increase in tissue content of cyclic AMP in the rat hepatic artery (Fig. 2a, b), the latter effect presumably reflecting activation of CGRP receptors on the vasculature. Both these effects were absent in arterial segments pretreated with capsaicin (Fig. 2a, b). However, pretreatment with capsaicin did not affect the cyclic AMP increase evoked by exogenous CGRP (Fig. 2b), which is consistent with capsaicin acting on sensory nerves. CGRP-like immunoreactive nerve fibres were visualized in the rat hepatic artery (Fig. 2c). Such nerves are also present in rat mesenteric[18] and guinea-pig basilar[19] arteries. Together, these findings support our proposal that CGRP released from perivascular sensory nerves mediates vasodilation by anandamide. The pronounced vasodilator effect of anandamide indicates that these nerves represent a powerful effector system for regulation of vascular tone.

To investigate the role of cannabinoid receptors in these vascular responses, we compared the effects of anandamide with those of a series of endogenous (palmitylethanolamide, 2-arachidonylglycerol) and synthetic (HU 210, WIN 55,212-2, CP 55,940) cannabinoid receptor agonists with varying selectivity for CB1 and CB2 receptors[1]. HU 210, WIN 55,212-2 and CP 55,940 are at least one order of magnitude more potent than anandamide as agonists of CB1 and CB2 receptors[1]. In rat hepatic and guinea-pig basilar arteries, palmitylethanolamide, HU 210 and WIN 55,212-2 did not produce any relaxation, whereas 2-arachidonylglycerol induced a small (rat hepatic artery) or inconsistent (guinea-pig basilar artery) relaxation at 10 μM (Fig. 3). CP 55,940 elicited significant relaxation in both arteries, but this effect was resistant to pretreatment with capsaicin and occurred only at a concentration of 10 μM (Fig. 3c, d). The failure of these different cannabinoid receptor agonists to mimic the action of anandamide indicates that CB1 or CB2 receptors do not mediate anandamide-induced vasorelaxation in these arteries.

The competitive CB1 receptor antagonist SR141716A (0.3 μM), which binds to this receptor with a K_i in the nanomolar range[1], did not attenuate the vasodilator responses to anandamide in rat hepatic (control: $pEC_{50} = 6.45 \pm 0.11$, $E_{max} = 100 \pm 1\%$; SR141716A: $pEC_{50} = 6.44 \pm 0.12$, $E_{max} = 97 \pm 1\%$; $n = 5$) and guinea-pig basilar (control: $pEC_{50} = 6.02 \pm 0.11$, $E_{max} = 92 \pm 3\%$; SR141716A: $pEC_{50} = 6.11 \pm 0.10$, $E_{max} = 91 \pm 2\%$; $n = 5$–8) arteries, and to methanandamide in the rat hepatic artery (control: $pEC_{50} = 6.50 \pm 0.08$, $E_{max} = 99 \pm 1\%$; SR141716A: $pEC_{50} = 6.30 \pm 0.04$, $E_{max} = 99 \pm 1\%$; $n = 5$). High concentrations of SR141716A (≥3 μM) can inhibit anandamide-induced relaxation in rat hepatic and mesenteric arteries, but the mechanism of this action is unclear[3,17]. Such high concentrations of SR141716A have effects unrelated to inhibition of CB1 or CB2 receptors[20,21]. This is also supported by this study, showing that the vasodilator response to capsaicin, which does not bind to CB1 receptors[22], is significantly inhibited by 10 μM SR141716A in the rat hepatic artery (control: $pEC_{50} = 8.37 \pm 0.13$, $E_{max} = 99 \pm 1\%$; SR141716A: $pEC_{50} = 7.42 \pm 0.12$, $E_{max} = 90 \pm 3\%$; $n = 4$).

It has been suggested that enzymatic cleavage of anandamide by a specific amidohydrolase to arachidonic acid and ethanolamine[22], with subsequent formation of vasodilator eicosanoids such as prostacyclin and eicosatrienoic acids, is responsible for the anandamide-induced

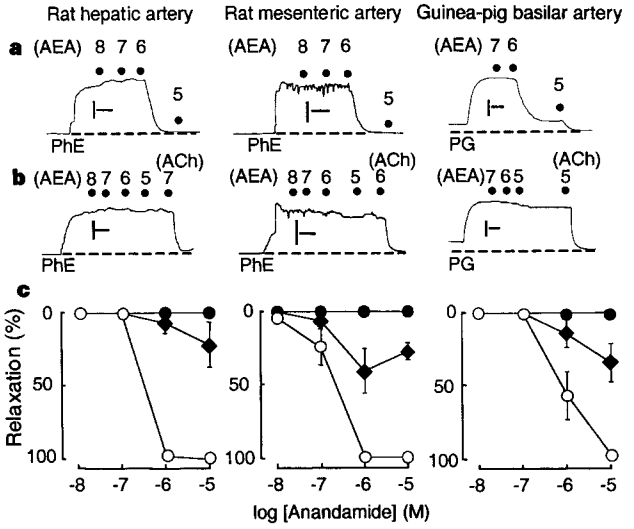

Figure 1 Effects of capsaicin and the CGRP receptor antagonist 8-37 CGRP on relaxations induced by anandamide (AEA) and acetylcholine (ACh) in rat and guinea-pig arteries. **a**, Typical relaxant responses to anandamide in these blood vessels contracted with phenylephrine (PhE; 1–3 μM) or prostaglandin $F_{2\alpha}$ (PG; 0.3–1 μM). Drug concentrations are given as –log molar concentrations. Horizontal and vertical scale markers represent 2 min and 2 mN, respectively. Dashed line indicates the basal tension level before addition of drugs. Each trace was obtained from a different arterial segment. **b**, Pretreatment with capsaicin (10 μM) for 1 h (followed by washout of capsaicin for 20 min) abolished the anandamide-induced relaxation, whereas subsequent application of acetylcholine (0.1–10 μM) always elicited complete relaxation (mediated by endothelium-derived hyperpolarising factor[2,3,24]) in 6 out of 6 rat hepatic, 4 out of 4 rat mesenteric and 5 out of 5 guinea-pig basilar arteries. **c**, Concentration–response curves for anandamide after treatment with capsaicin (10 μM; filled circles), 8-37 CGRP (2 μM; diamonds) for 30 min or vehicle (circles) in the different arteries ($n = 5$–8).

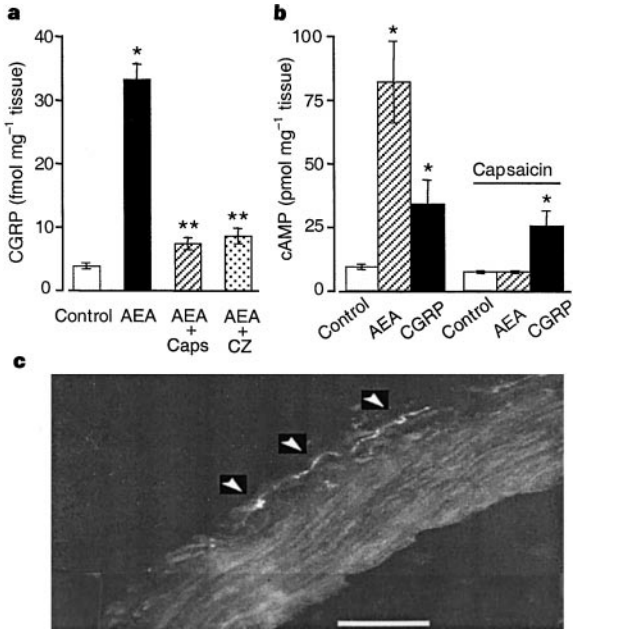

Figure 2 Release of CGRP from sensory nerves and effects of anandamide (AEA) and CGRP on cAMP levels in the rat hepatic artery. **a**, The effect of 10 min exposure to anandamide (10 μM) on CGRP release was measured in untreated vessels ($n = 11$) and in vessels pretreated with capsaicin (Caps; 10 μM, $n = 4$), followed by washout of capsaicin for 20 min, or incubated with capsazepine (CZ; 10 μM, 20 min, $n = 5$). Control refers to preparations exposed to vehicle ($n = 6$). **b**, cAMP contents were measured after 5 min in the absence (control) or presence of either anandamide (AEA; 10 μM) or CGRP (10 nM) before and after pretreatment with capsaicin as above ($n = 6$). * $P < 0.05$ compared to controls, ** $P < 0.05$ compared to anandamide alone. **c**, CGRP-like immunoreactive nerve fibres were observed in the adventitia. Bar, 40 μm.

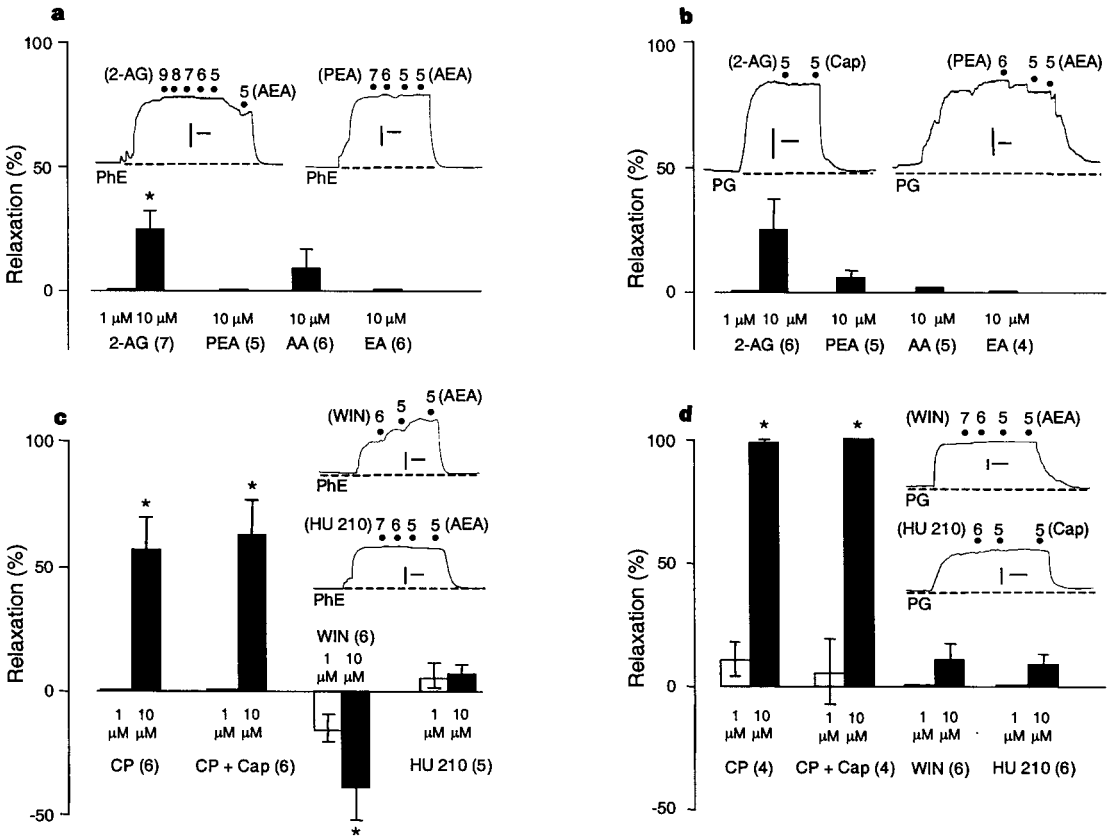

Figure 3 Relaxant effects of endogenous and synthetic cannabinoid receptor agonists in rat hepatic and guinea-pig basilar arteries. **a**, **b**, Effects of the endocannabinoids 2-arachidonylglycerol (2-AG) and palmitylethanolamide (PEA), and arachidonic acid (AA) and ethanolamine (EA), which are breakdown products of anandamide, in (**a**) rat hepatic and (**b**) guinea-pig basilar arteries contracted with phenylephrine (PhE; 1–3 μM) or prostaglandin $F_{2\alpha}$ (PG; 0.1–1 μM), respectively. Anandamide (AEA; 10 μM) and capsaicin (Cap; 10 μM) completely relaxed the vessels. Drug concentrations are given as –log molar concentrations. Horizontal and vertical scale markers represent 2 min and 2 mN, respectively. Dashed line indicates the basal tension level before addition of drugs. Each trace was obtained from a different arterial segment. **c**, **d**, Among the synthetic compounds tested (HU 210, WIN 55,212-2 and CP 55,940), only CP 55,940 caused relaxation in (**c**) rat hepatic and (**d**) guinea-pig basilar arteries. In contrast to anandamide, CP 55,940 also relaxed arteries after treatment with capsaicin (10 μM). Anandamide (10 μM) or capsaicin (10 μM) relaxed vessels exposed to HU 210 and WIN 55,212-2. The number of experiments is shown in brackets. $^*P < 0.05$ compared to vehicle (0.2% ethanol).

relaxation in bovine coronary artery[20]. However, this relaxation is endothelium-dependent, in contrast to the vasodilator response to anandamide in rat hepatic[3] and mesenteric[17] and guinea-pig basilar (unpublished observations) arteries. Cyclo-oxygenase products can be ruled out in this study, as indomethacin was present in all experiments, and eicosatrienoic acids cannot relax rat hepatic[23] and guinea-pig basilar[24] arteries. Furthermore, arachidonic acid (10 μM) and ethanolamine (10 μM) had no effect in these arteries (Fig. 3a, b), whereas methanandamide, which is resistant to enzymatic hydrolysis[1], was at least as potent as anandamide as a vasodilator in rat hepatic (methanandamide: $pEC_{50} = 6.53 \pm 0.08$, $E_{max} = 97 \pm 1\%$; $n = 8$; anandamide: $pEC_{50} = 6.49 \pm 0.01$, $E_{max} = 100 \pm 1\%$; $n = 6$) and mesenteric[21] arteries. These findings indicate that anandamide itself is responsible for the vasodilator activity.

Capsaicin and other vanilloid compounds act by binding to specific vanilloid receptors on primary sensory neurons. Molecular studies have shown that the cloned vanilloid receptor (VR1) is a calcium-permeable, non-selective cation channel that is gated by noxious heat or extracellular protons[8]. In addition to these physiological stimuli, VR1 might also be modulated by endogenous, capsaicin-like substances, such as endocannabinoids or other lipids. Olvanil (but not capsaicin) binds to both the anandamide transporter and the CB1 receptor, indicating that capsaicin-like compounds and endocannabinoids can indeed recognize the same proteins[22]. VR1 is closely related to members of the transient receptor potential (TRP) channel family[8]. Membrane-derived second messengers, such as diacylglycerol or arachidonic acid, can activate certain TRP-channel subtypes at micromolar concentrations[25,26]. To determine whether anandamide interacts with native vanilloid receptors, we examined the effect of capsazepine, a competitive vanilloid receptor antagonist[6,7], on the vasodilator responses to anandamide, methanandamide and capsaicin. As shown in rat hepatic and mesenteric and guinea-pig basilar arteries, capsazepine significantly inhibits the vasodilator effects of anandamide and capsaicin (Fig. 4a). Capsazepine also suppresses the anandamide-induced release of CGRP from capsaicin-sensitive nerves (Fig. 2a). Further experiments on the rat hepatic artery showed that capsazepine produces a rightward parallel shift of the concentration–response curves for both capsaicin and methanandamide without affecting the maximal response, consistent with a competitive mode of inhibition (Fig. 4b, c). The Schild plots for capsazepine using capsaicin and methanandamide as agonists were not significantly different, and revealed pA_2 values (mean ± s.d.) of 6.24 ± 0.14 and 6.34 ± 0.06, respectively (Fig. 4d), strongly favouring an identical site of action for these agonists.

To exclude the possibility that anandamide causes relaxation by activating neuronal calcium channels, we examined the effects of nimodipine and the ω-conotoxins GVIA and MVIIC, inhibitors of L-, N- and P/Q-type calcium channels[27], on the vasodilator response to anandamide in the rat hepatic artery. Neither ω-conotoxin GVIA (0.1 μM) plus MVIIC (0.1 μM) nor nimodipine (0.1 μM) in combination with these toxins inhibited the anandamide-induced vasodilation (control: $pEC_{50} = 6.56 \pm 0.09$, $E_{max} = 98 \pm 1\%$, $n = 6$; ω-conotoxin GVIA and MVIIC: $pEC_{50} = 6.58 \pm 0.08$;

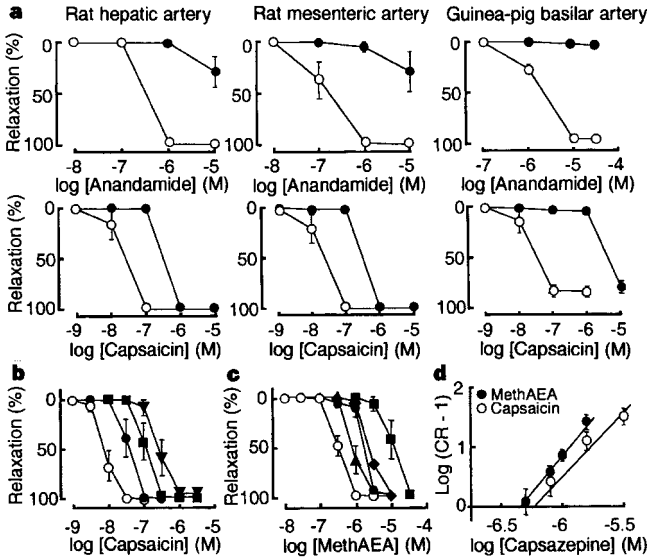

Figure 4 Effect of the vanilloid receptor antagonist capsazepine on relaxations elicited by anandamide, methanandamide and capsaicin in rat and guinea-pig arteries. **a**, Concentration–response curves for anandamide ($n = 5$–6) and capsaicin ($n = 5$–6) after incubation with capsazepine (3 μM) for 30 min (filled circles) or vehicle (open circles; 0.3% ethanol) in arteries contracted with phenylephrine (PhE; 1–3 μM) or prostaglandin $F_{2\alpha}$ (PG; 0.1-1 μM). **b**, **c**, Concentration–response curves for capsaicin ($n = 6$) and methanandamide (MethAEA; $n = 5$–7) in the absence (open circles) and presence of various concentrations of capsazepine (0.5 μM, upward triangles; 0.8 μM, filled circles; 1.0 μM, diamonds; 1.6 μM, squares; 3.2 μM, downward triangles) in rat hepatic arteries. **d**, Schild plots for capsazepine, using capsaicin (open circles) or methanandamide (filled circles) as agonists. For clarity, the individual data points are summarized as mean ± s.e.m. (vertical lines; $n = 5$–8). The slopes of the regression lines for capsaicin and methanandamide were (mean ± s.d.) 2.12 ± 0.36 and 2.41 ± 0.32, respectively.

$E_{max} = 99 \pm 1\%$, $n = 6$; nimodipine and ω-conotoxin GVIA and MVIIC: $pEC_{50} = 6.31 \pm 0.02$, $E_{max} = 93 \pm 3\%$, $n = 5$). α-Latrotoxin is a neurotoxin that causes neurotransmitter release after binding to presynaptic nerve terminals[28]. The vasodilator response to α-latrotoxin (1 nM) was unaffected by capsazepine (3 μM), but abolished by CGRP 8-37 (2 μM) or capsaicin pretreatment in the rat hepatic artery (control: 98 ± 1%, $n = 12$; capsazepine: 93 ± 2%; $n = 6$; CGRP 8-37: −8 ± 3%, $n = 6$; capsaicin: −16 ± 8%, $n = 7$). This indicates that capsazepine does not act through depletion of neurotransmitters from sensory nerves. Furthermore, capsazepine (3 μM) had no effect on the CGRP-induced relaxation in rat hepatic (control: $pEC_{50} = 9.46 \pm 0.01$, $E_{max} = 100 \pm 1\%$; capsazepine: $pEC_{50} = 9.39 \pm 0.04$, $E_{max} = 100 \pm 1\%$, $n = 6$), mesenteric (control: $pEC_{50} = 10.4 \pm 0.04$, $E_{max} = 99 \pm 1\%$; capsazepine: $pEC_{50} = 10.3 \pm 0.12$, $E_{max} = 99 \pm 1\%$, $n = 4$) and guinea-pig basilar (control: $pEC_{50} = 8.72 \pm 0.16$, $E_{max} = 98 \pm 1\%$; capsazepine: $pEC_{50} = 8.70 \pm 0.15$, $E_{max} = 99 \pm 1\%$, $n = 4$–5) arteries, confirming the specificity of capsazepine.

To obtain direct evidence that anandamide interacts with vanilloid receptors, we examined the effects of anandamide and other lipid messengers on the cloned VR1 channel. Whole-cell patch-clamp recordings from VR1-transfected HEK293 cells showed robust membrane currents when anandamide was applied by bath perfusion (Fig. 5a, top left); such currents were not observed in vector-transfected HEK293 cells ($n = 5$; data not shown). Similar responses were seen with inside-out membrane patches excised from VR1-expressing *Xenopus* oocytes (Fig. 5a, top, middle), but not uninjected oocytes ($n = 4$; not shown). In each case, anandamide elicited outwardly rectifying cationic currents characteristic of VR1 (Fig. 5a, bottom). In VR1-transfected HEK293 cells, pEC_{50} for anandamide was estimated as 5.31 ± 0.06 ($n = 13$). Thus, anandamide

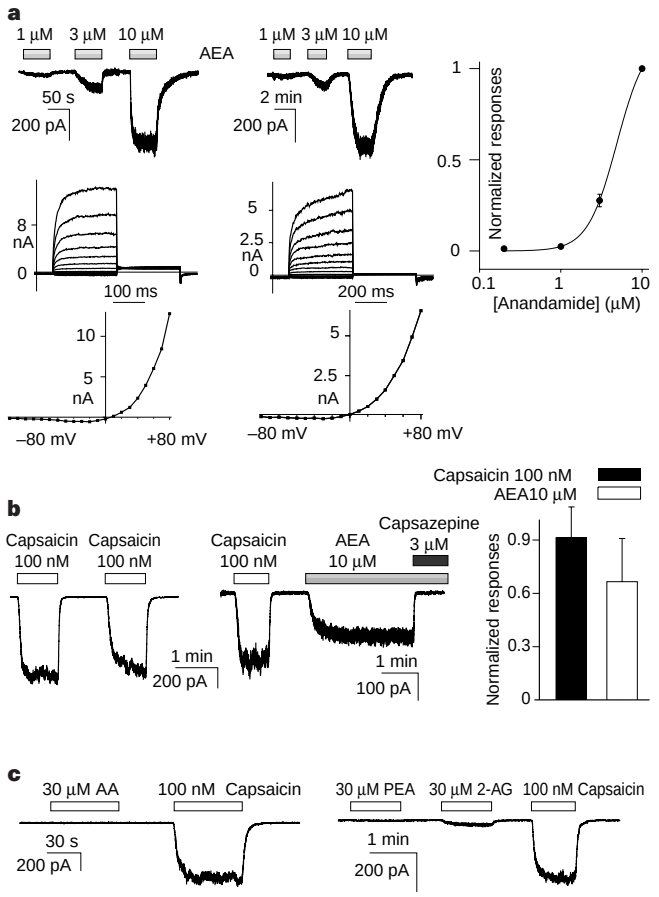

Figure 5 Anandamide activates the cloned vanilloid receptor (VR1). **a**, Patch-clamp recordings from VR1-expressing HEK293 cells (top left, whole-cell configuration) or *Xenopus* oocytes (top middle, excised inside-out membrane patch) show concentration-dependent responses to bath-applied anandamide (plotted for VR1-transfected HEK293 cells, top right; $n = 6$–24). The curve fit revealed a Hill coefficient for anandamide of 2.41 ± 0.46, which is close to that obtained for capsaicin in VR1-transfected *Xenopus* oocytes (2.08) (ref. 8). Current–voltage relationships for responses in HEK293 cells or oocytes (bottom left and right, respectively) showed pronounced outward rectification characteristic of VR1 in the presence of anandamide (10 μM). Currents were generated by stepping from a holding potential of –80 mV to the test potentials as indicated in the figure. **b**, Relative responses of VR1 to capsaicin ($n = 7$) and anandamide (AEA; $n = 11$) were determined by whole-cell patch-clamp analysis of VR1-expressing HEK293 cells. Currents were normalized to an initial response to 100 nM capsaicin. Anandamide-evoked currents were inhibited by co-application of 3 μM capsazepine ($n = 8$). **c**, VR1-expressing HEK293 cells did not respond to arachidonic acid (AA; $n = 8$) or palmitylethanolamide (PEA; $n = 9$), whereas small membrane currents were elicited by 2-arachidonylglycerol (2-AG; $n = 9$).

is at least as potent on VR1 as other lipid messengers on *Drosophila* or mammalian TRP channels[25,26]. At a near maximal concentration (10 μM), anandamide evoked a response similar to that obtained with 100 nM capsaicin (Fig. 5b). Relative to capsaicin, the efficacy of anandamide as a VR1 agonist was estimated as 30–50%. Anandamide (10 μM) was unable to induce membrane currents in HEK293 cells expressing cloned serotonin-gated (5-HT_3R-A, $n = 6$; data not shown) or ATP-gated ($P2X_2$, $n = 7$; data not shown) ion channels, whereas these transfected cells consistently responded to 10 μM serotonin (current range, 0.5–2 nA) or 10 μM ATP (current range, 4–7 nA), providing additional proof that anandamide interacts specifically with VR1. The observation that capsazepine completely and rapidly antagonized anandamide-induced currents further supports this conclusion (Fig. 5b). In VR1-expressing HEK293 cells, neither arachidonic acid nor

palmitylethanolamide evoked significant inward current responses, and 2-arachidonylglycerol elicited only a small current when applied at a concentration of 30 μM (Fig. 5c). Diacylglycerol activates human TRPC3 and TRPC6, but not rat VR1 channels[26]. Together, these observations show that anandamide, but not all lipids, can activate VR1.

Although capsaicin was a more potent agonist than anandamide or methanandamide in all our test systems, the absolute potencies of these compounds were always higher (3–30-fold) in the vascular preparations than in VR1-expressing HEK293 cells and *Xenopus* oocytes[8,29]. The reason for the difference in sensitivity to vanilloid receptor agonists between these test systems is unclear, but obvious possibilities are the presence in intact tissues of large receptor reserves, effective cellular amplification systems and/or potential VR1 channel regulators, which are absent in heterologous expression systems. Such differences may also account for the observation that, although methanandamide and anandamide are equally effective as vasodilators, methanandamide is only about 10% as effective as anandamide in producing membrane currents in HEK293 cells expressing VR1 (data not shown).

Our findings indicate that anandamide activates vanilloid receptors on primary sensory neurons, and provide a likely molecular mechanism for the non-CB1 receptor-mediated vasodilator action of anandamide. This raises the possibility that anandamide and/or structurally-related lipids act as endogenous vanilloid receptor modulators and thereby participate in the regulation of the various afferent (nociception, visceral reflexes) and efferent (for example local vasodilation and neurogenic inflammation) functions subserved by capsaicin-sensitive sensory neurons. □

Methods

Recording of tension. Experiments were performed on hepatic (400 μm outer diameter) and mesenteric (200 μm outer diameter) arteries from female Wistar–Hannover rats (200–250 g) and on basilar arteries (300 μm outer diameter) from male guinea-pigs (300 g). The arteries were cut into ring segments and mounted in tissue baths containing aerated physiological salt solution (5% CO_2 and 95% O_2; 37 °C; pH 7.4) as described[3,24]. We carried out all experiments in the presence of N^G-nitro-L-arginine (0.3 mM) and indomethacin (10 μM) to eliminate any contribution of nitric oxide and cyclooxygenase products, respectively. We studied relaxant responses in preparations contracted with phenylephrine (rat hepatic and mesenteric arteries) or prostaglandin $F_{2\alpha}$ (guinea-pig basilar artery)[3,24]. When stable contractions were obtained, agonists were added cumulatively to determine concentration–response relationships.

Measurements of CGRP and cyclic AMP. Segments of rat hepatic arteries were equilibrated for 1 h in aerated physiological salt solution (5% CO_2 and 95% O_2; 37 °C; pH 7.4), containing N^G-nitro-L-arginine (0.3 mM) and indomethacin (10 μM). CGRP: preparations were transferred to eppendorff tubes, containing physiological salt solution with the addition of 0.05% BSA and the test drugs. The segments were removed after 5 min, and the solution in the test tubes was evaporated. We determined the amount of CGRP in the pellet using rat ^{125}I-CGRP radioimmunoassay RIA kit (Peninsula labs). The amount of cyclic AMP after 5 min exposure to the test drugs was determined as described[30].

Immunohistochemistry. Rat hepatic arteries were fixed in 4% formaldehyde for 4 h, rinsed in a phosphate buffer (pH 7.4) containing 15% sucrose for three days and then frozen. Cryostat sections were cut at a thickness of 10 μm and prepared for reaction with CGRP antiserum (EURO-DIAGNOSTICA, Malmö, Sweden) at 1:320 dilution for 24 h (room temperature). CGRP-like immunoreactivity was visualized after exposure to FITC-conjugated goat anti-guinea-pig IgG (Sigma, USA) at 1:80 dilution for 90 min.

Patch-clamp. HEK293 cells were transfected with 0.5 μg VR1 cDNA, using lipofectamine (Gibco), and plated on glass coverslips 24–72 h before analysis. *Xenopus* oocytes were prepared as described[8] and injected with 2.5 ng of VR1 cRNA. Standard bath solution for all recordings contained (in mM): 10 Tris, 150 CsCl, 1 $MgCl_2$, 1 EGTA, pH 7.4. For oocyte patch recording, this solution was also included in the pipette, whereas for whole-cell recording from HEK293 cells, the pipette contained a 0.9 times dilution of this solution. For all continuous recordings, the membrane was held at −40 mV. All experiments were done at room temperature. Drugs were prepared as ethanol stocks and diluted with bath solution, containing 0.2 mM beta-cyclodextrin, and this solution was bath sonicated for 5 min in ice water before use. Agonist washout was achieved with bath solution, containing 0.2 mM beta-cyclodextrin.

Calculations and statistics. Relaxations are expressed as percentage reversal of the agonist-induced contraction (100% indicates a complete relaxation). We calculated drug concentrations eliciting 50% (EC_{50}) and maximal (E_{max}) relaxation as described[24]. Data are presented as means ± s.e.m. (vertical lines in Figures), and *n* indicates the number of vascular segments (animals) or cells examined. pA_2 and slope values of the Schild plots were estimated according to the Jackknife method. Statistical analysis was performed by using Student's *t*-test, Mann–Whitney *U*-test or analysis of variance (ANOVA), followed by Bonferroni Dunn's post hoc test (Statview 4.12). Cyclic AMP values were log transformed. Statistical significance was accepted when $P < 0.05$.

Drugs. Anandamide, R(+)-methanandamide, 2-arachidonylglycerol, WIN 55,212-2 (RBI); HU 210, CP 55,940 (Tocris); palmitylethanolamide (Biomol); capsaicin, capsazepine (Fluka); SR141716A (Sanophi Winthrop); arachidonic acid (Sigma) were all dissolved in ethanol. Distilled water was used as solvent for acetylcholine chloride, L-phenylephrine hydrochloride, N^G-nitro-L-arginine, human 8-37 CGRP, ethanolamine hydrochloride (Sigma); human α-CGRP (Peninsula); α-latrotoxin, ω-conotoxins GVIA and MVIIC (Alomone); prostaglandin $F_{2\alpha}$ (Upjohn); indomethacin (Confortid, Dumex). Nimodipine (Nimotop, Bayer) was diluted with saline.

Received 18 March; accepted 21 June 1999.

1. Pertwee, R. G. Pharmacology of cannabinoid CB_1 and CB_2 receptors. *Pharmacol. Ther.* **74,** 129–180 (1997).
2. Plane, F., Holland, M., Waldron, G. J., Garland, C. J. & Boyle, J. P. Evidence that anandamide and EDHF act via different mechanisms in rat isolated mesenteric arteries. *Br. J. Pharmacol.* **121,** 1509–1511 (1997).
3. Zygmunt, P. M. *et al.* Studies on the effects of anandamide in rat hepatic artery. *Br. J. Pharmacol.* **122,** 1679–1686 (1997).
4. Wagner, J. A., Varga, K., Jarai, Z. & Kunos, G. Mesenteric vasodilation mediated by endothelial anandamide receptors. *Hypertension* **33,** 429–434 (1999).
5. Han, S.-P., Naes, L. & Westfall, T. C. Inhibition of periarterial nerve stimulation-induced vasodilation of the mesenteric arterial bed by CGRP (8-37) and CGRP receptor desensitization. *Biochem. Biophys. Res. Commun.* **168,** 786–791 (1990).
6. Bevan, S. *et al.* Capsazepine: a competitive antagonist of the sensory neurone excitant capsaicin. *Br. J. Pharmacol.* **107,** 544–552 (1992).
7. Szallasi, A. & Blumberg, P. M. Vanilloid (capsaicin) receptors and mechanisms. *Pharmacol. Rev.* **51,** 159–212 (1999).
8. Caterina, M. J. *et al.* The capsaicin receptor: a heat-activated ion channel in the pain pathway. *Nature* **389,** 816–824 (1997).
9. Devane, W. A. *et al.* Isolation and structure of a brain constituent that binds to the cannabinoid receptor. *Science* **258,** 1946–1949 (1992).
10. Deutsch, D. G. *et al.* Production and physiological actions of anandamide in the vasculature of the rat kidney. *J. Clin. Invest.* **100,** 1538–1546 (1997).
11. Di Marzo, V., De Petrocellis, L., Sepe, N. & Buono, A. Biosynthesis of anandamide and related acylethanolamides in mouse J774 macrophages and N_{18} neuroblastoma cells. *Biochem. J.* **316,** 977–984 (1996).
12. Varga, K., Lake, K. D., Huangfu, D., Guyenet, P. G. & Kunos, G. Mechanism of the hypotensive action of anandamide in anesthetized rats. *Hypertension* **28,** 682–686 (1996).
13. Wagner, J. A. *et al.* Activation of peripheral CB_1 cannabinoid receptors in haemorrhagic shock. *Nature* **390,** 518–521 (1997).
14. Varga, K., Wagner, J. A., Bridgen, D. T. & Kunos, G. Platelet- and macrophage-derived endogenous cannabinoids are involved in endotoxin-induced hypotension. *FASEB J.* **12,** 1035–1044 (1998).
15. Ishac, E. J. N. *et al.* Inhibition of exocytotic noradrenaline release by presynaptic cannabinoid CB_1 receptors on peripheral sympathetic nerves. *Br. J. Pharmacol.* **118,** 2023–2028 (1996).
16. Sugiura, T. *et al.* Detection of an endogenous cannabimimetic molecule 2-arachidonoylglycerol, and cannabinoid CB1 receptor mRNA in human vascular cells: is 2-arachidonoylglycerol a possible vasomodulator? *Biochem. Biophys. Res. Commun.* **243,** 838–843 (1998).
17. White, R. & Hiley, C. R. The actions of some cannabinoid receptor ligands in the rat isolated mesenteric artery. *Br. J. Pharmacol.* **125,** 533–541 (1998).
18. Kawasaki, H., Takasaki, K., Saito, A. & Goto, K. Calcitonin gene-related peptide acts as a novel vasodilator neurotransmitter in mesenteric resistance vessels of the rat. *Nature* **335,** 164–167 (1988).
19. Edvinsson, L., Ekman, R., Jansen, I., McCulloch, J. & Uddman, R. Calcitonin gene-related peptide and cerebral blood vessels: distribution and vasomotor effects. *J. Cereb. Blood Flow Metab.* **7,** 720–728 (1987).
20. Pratt, P. F., Hillard, C. J., Edgemond, W. S. & Campbell, W. B. *N*-arachidonylethanolamide relaxation of bovine coronary artery is not mediated by CB1 cannabinoid receptor. *Am. J. Physiol.* **274,** H375–H381 (1998).
21. White, R. & Hiley, C. R. The actions of the cannabinoid receptor antagonist, SR 141716A, in the rat isolated mesenteric artery. *Br. J. Pharmacol.* **125,** 689–696 (1998).
22. Di Marzo, V. *et al.* Interactions between synthetic vanilloids and the endogenous cannabinoid system. *FEBS Lett.* **436,** 449–454 (1998).
23. Zygmunt, P. M., Edwards, G., Weston, A. H., Davis, S. C. & Högestätt, E. D. Effects of cytochrome P450 inhibitors on EDHF-mediated relaxation in the rat hepatic artery. *Br. J. Pharmacol.* **118,** 1147–1152 (1996).
24. Petersson, J., Zygmunt, P. M., Jönsson, P. & Högestätt, E. D. Characterization of endothelium-dependent relaxation in guinea pig basilar artery—effects of hypoxia and role of cytochrome P_{450} mono-oxygenase. *J. Vasc. Res.* **35,** 285–294 (1998).
25. Chyb, S., Raghu, P. & Hardie, R. Polyunsaturated fatty acids activate the drosophila light-sensitive channels TRP and TRPL. *Nature* **397,** 255–259 (1999).

26. Hofmann, T. *et al.* Direct activation of human TRPC6 and TRPC3 channels by diacylglycerol. *Nature* **397,** 259–263 (1999).
27. Olivera, B. M., Miljanich, G. P., Ramachandran, J. & Adams, M. E. Calcium channel diversity and neurotransmitter release: the omega-conotoxins and omega-agatoxins. *Annu. Rev. Biochem.* **63,** 823–867 (1994).
28. Geppert, M. *et al.* Neurexin Ia is a major α-latrotoxin receptor that cooperates in α-latrotoxin action. *J. Biol. Chem.* **273,** 1705–1710 (1998).
29. Tominaga, M. *et al.* The cloned capsaicin receptor integrates multiple pain-producing stimuli. *Neuron* **21,** 531–543 (1998).
30. Zygmunt, P. M., Grundemar, L. & Högestätt, E. D. Endothelium-dependent relaxation resistant to Nω-nitro-L-arginine in the rat hepatic artery and aorta. *Acta Physiol. Scand.* **152,** 107–114 (1994).

Acknowledgements. This work was supported by the Swedish Medical Research Council, the Medical Faculty of Lund (ALF) and the Crafoords Foundation (E.D.H.), the National Institutes of Health and the McKnight Foundation for Neuroscience (H.C. and D.J.) and the Ministero dell Universita e dela Ricerca Scientifica (V.D.M.). P.M.Z. was supported by the Swedish Society for Medical Research and the Swedish Medical Research Council. J.P. was supported by the Medical Faculty of Lund (ALF).

Correspondence and requests for materials should be addressed to E.D.H. (e-mail: Edward.Hogestatt@klinfarm.lu.se).

Munc13-1 is essential for fusion competence of glutamatergic synaptic vesicles

Iris Augustin*, Christian Rosenmund†, Thomas C. Südhof‡ & Nils Brose*

* *Max-Planck-Institut für Experimentelle Medizin, AG Molekulare Neurobiologie, Hermann-Rein-Str. 3, D-37075 Göttingen, Bundesrepublik Deutschland*
† *Max-Planck-Institut für Biophysikalische Chemie, Abteilung Membranbiophysik, Am Faßberg 11, D-37077 Göttingen, Bundesrepublik Deutschland*
‡ *Center for Basic Neuroscience, Department of Molecular Genetics, Howard Hughes Medical Institute, University of Texas Southwestern Medical Center, 5323 Harry Hines Blvd, Dallas, Texas 75235, USA*

Neurotransmitter release at synapses between nerve cells is mediated by calcium-triggered exocytotic fusion of synaptic vesicles[1]. Before fusion, vesicles dock at the presynaptic release site where they mature to a fusion-competent state[1,2]. Here we identify Munc13-1, a brain-specific presynaptic phorbol ester receptor[3,4], as an essential protein for synaptic vesicle maturation. We show that glutamatergic hippocampal neurons from mice lacking Munc13-1 form ultrastructurally normal synapses whose synaptic-vesicle cycle is arrested at the maturation step. Transmitter release from mutant synapses cannot be triggered by action potentials, calcium-ionophores or hypertonic sucrose solution. In contrast, release evoked by α-latrotoxin is indistinguishable from wild-type controls, indicating that the toxin can bypass Munc13-1-mediated vesicle maturation. A small subpopulation of synapses of any given glutamatergic neuron as well as all synapses of GABA (γ-aminobutyric acid)-containing neurons are unaffected by Munc13-1 loss, demonstrating the existence of multiple and transmitter-specific synaptic vesicle maturation processes in synapses.

Deletion mutations in the mouse gene for Munc13-1 were generated by homologous recombination in embryonic stem cells. Munc13-1-deficient mice do not feed and are distinguishable from wild-type animals shortly after birth by a lack of milk in their stomachs, weakness and reduced breathing rate. Mutant mice die within a few hours of birth. Anatomical and morphological analyses of newborn offspring from heterozygous interbreedings showed that the overall structure and cytoarchitecture of mutant brains and the distribution of synaptic markers (synaptotagmin, synapsin) were indistinguishable from those of wild-type controls (data not shown). Immunoblotting of brains from newborn littermates showed that, in addition to Munc13-1, which was completely absent in mutant mice, 4 out of 35 pre- and postsynaptic proteins tested showed small changes (complexin I, 82 ± 8%; Rab3A, 76 ± 9%; Munc13-1-interactor syntaxin IA/B, 85 ± 5%; synaptobrevin/VAMP II, 128 ± 6% of wild-type control). In contrast, the levels of other Munc13 isoforms (Munc13-2 and Munc13-3) were not changed in mutant brains (see Supplementary Information).

To determine the role of Munc13-1 in synaptic transmission, we performed electrophysiological analyses of cultured hippocampal neurons from newborn pups. Routinely, recordings were done on single hippocampal neurons that were cultured on microdot islands where they form recurrent (autaptic) synapses onto themselves. Cultures obtained from wild-type and mutant hippocampi did not differ in overall morphology and cell density. However, whole-cell patch-clamp analysis revealed a marked phenotypical change in Munc13-1-deficient cultures. Although wild-type and heterozygous hippocampal neurons showed similar robust excitatory postsynaptic responses upon evoked release (1.43 ± 0.43 nA for +/+, $n = 50$; 1.58 ± 0.25 nA for +/–, $n = 48$), synaptic responses in mutant cells were reduced by more than 90% (0.11 ± 0.01 nA, $n = 134$; Fig. 1a, c). This was not due to a change in the density of voltage-gated conductances, as mutant cells generated normal action potentials in response to current injections, and their sodium, potassium and calcium current densities were not significantly different from normal (not shown). Inhibitory GABA-mediated transmission measured in cells from the same cultures appeared to be unaffected by the lack of Munc13-1 (1.93 ± 0.56 nA in +/+, $n = 11$; 1.91 ± 0.19 nA in +/–, $n = 59$; versus 1.85 ± 0.14 nA in –/–, $n = 74$; Fig. 1b, c). To test whether the abnormalities in glutamatergic transmission in Munc13-1-deficient cells are caused by a selective deficiency in, or lack of, voltage-gated calcium channels in mutant synapses, we used the calcium ionophore calcimycin to bypass presynaptic voltage-gated calcium channels. In wild-type neurons, addition of calcimycin triggered robust miniature excitatory postsynaptic current (mEPSC) bursts (postsynaptic peak amplitude 0.374 ± 0.083 nA, $n = 7$) that were abolished by the glutamate receptor blocker NBQX (2,3-dihydroxy-6-nitro-7-sulphamoylbenzene quinoxaline). In contrast, Munc13-1-deficient cells responded weakly (0.017 ± 0.007 nA, $n = 9$) (Fig. 1d, e), showing that changes in calcium influx cannot explain the mutant phenotype. The observed specific reduction in glutamatergic transmission was not due to loss of synapses, as the density of total synaptic contacts (not shown) and the density of glutamatergic synapses were not altered by the mutation (Fig. 1f).

Given that synapses form at normal densities in Munc13-1-deficient neuronal cultures (Fig. 1f) and that mutant neurons generate normal action potentials, the marked and specific reduction in evoked excitatory synaptic responses resulting from loss of Munc13-1 could be caused by either a defect in the presynaptic release machinery, or an alteration in postsynaptic sensitivity. From the following results, we conclude that the postsynaptic glutamate-receptor sensitivity of hippocampal neurons was not affected by the Munc13-1 mutation: mEPSC amplitudes and their probability density were not changed in mutant cells as compared to wild-type controls (14.6 ± 1.2 pA, $n = 465$, five –/– cells versus 15.1 ± 1.5 pA, $n = 523$, five +/+ cells), and responses to exogenous application of glutamatergic agonists were identical in mutant and wild-type neurons. Responses evoked by 30 μM kainate resulted in inward currents of 1.47 ± 0.4 nA ($n = 6$) and 1.87 ± 0.69 nA ($n = 6$) for wild-type and –/– neurons, respectively. NMDA (*N*-methyl-D-aspartate) responses (10 μM) were 2.02 ± 0.31 nA (wild type, $n = 5$) versus 1.75 ± 0.23 (–/–, $n = 12$). Furthermore, expression of the postsynaptic NMDA receptor isoform NMDA R1 was not altered in Munc13-1 mutant brains (see Supplementary Information).

Because mutant neurons showed normal action potentials and postsynaptic sensitivity, and because Munc13-1 is specifically localized to presynaptic active zones in rat hippocampus[4], presynaptic mechanisms are the most likely cause for the aberrant phenotype of Munc13-1-deficient neurons. In principle, these mechanisms